

Incommensurate Spin Ordering and Fluctuations in underdoped $\text{La}_{2-x}\text{Ba}_x\text{CuO}_4$

S. R. Dunsiger,¹ Y. Zhao,¹ Z. Yamani,² W. J. L. Buyers,^{2,3} H. Dabkowska,¹ and B. D. Gaulin^{1,3}

¹*Department of Physics and Astronomy, McMaster University, Hamilton, Ontario, L8S 4M1, Canada.*

²*Canadian Neutron Beam Centre, NRC, Chalk River Laboratories, Chalk River, Ontario, K0J 1J0, Canada*

³*Canadian Institute for Advanced Research, 180 Dundas St. W., Toronto, Ontario, M5G 1Z8, Canada*

(Dated: October 27, 2018)

Using neutron scattering techniques, we have studied incommensurate spin ordering as well as low energy spin dynamics in single crystal underdoped $\text{La}_{2-x}\text{Ba}_x\text{CuO}_4$ with $x \sim 0.095$ and 0.08 ; high temperature superconductors with $T_C \sim 27$ K and 29 K respectively. Static two dimensional incommensurate magnetic order appears below $T_N = 39.5 \pm 0.3$ K in $\text{La}_{2-x}\text{Ba}_x\text{CuO}_4$ ($x=0.095$) and a similar temperature for $x=0.08$ within the low temperature tetragonal phase. The spin order is unaffected by either the onset of superconductivity or the application of magnetic fields of up to 7 Tesla applied along the c -axis in the $x=0.095$ sample. Such magnetic field *independent* behaviour is in marked contrast with the field induced enhancement of the staggered magnetisation observed in the related $\text{La}_{2-x}\text{Sr}_x\text{CuO}_4$ system, indicating this phenomenon is not a universal property of cuprate superconductors. Surprisingly, we find that incommensurability δ is only weakly dependent on doping relative to $\text{La}_{2-x}\text{Sr}_x\text{CuO}_4$. Dispersive excitations in $\text{La}_{2-x}\text{Ba}_x\text{CuO}_4$ ($x=0.095$) at the same incommensurate wavevector persist up to at least 60 K. The dynamical spin susceptibility of the low energy spin excitations saturates below T_C , in a similar manner to that seen in the superconducting state of $\text{La}_2\text{CuO}_{4+y}$.

PACS numbers: 75.25.+z, 74.72.Dn, 75.30.Ds

The roles of spin, charge and lattice degrees of freedom have been central to the rich behaviour brought to light over the last 20 years in superconducting lamellar copper oxides^{1,2,3}. In particular, the cuprates exhibit phenomena which are a sensitive function of doping, evolving from an antiferromagnetic insulating parent compound into a superconducting phase with increasing hole density. A heterogeneous electronic phase composed of stripes of itinerant charges now appears to be a generic feature of hole doped ternary transition metal oxides⁴ such as manganites^{5,6} and nickelates^{7,8,9}, as well as cuprates. The explanation for these incommensurate spin ordered states is the subject of ongoing debate. In an itinerant picture, the spin dynamics are described in terms of electron-hole pair excitations about an underlying Fermi surface^{11,12,13}. Alternatively, within the stripe picture of doped, two dimensional Mott insulators, the non-magnetic holes in these materials organize into quasi-one dimensional stripes which separate antiferromagnetic insulating antiphase domains¹⁴. Adjacent antiferromagnetic regions are π out of phase with each other giving rise to a magnetic structure with incommensurate periodicity, where the supercell dimension is twice the hole stripe periodicity.

The static spin structures in the undoped, parent compounds such as La_2CuO_4 ¹⁵ or $\text{YBa}_2\text{Cu}_3\text{O}_6$ ¹⁶ have been determined by neutron scattering to be relatively simple two sublattice antiferromagnets characterized by a commensurate ordering wavevector of $(0.5, 0.5)$ in reciprocal lattice units within the tetragonal basal plane. On hole doping with either Sr substituting for La in $\text{La}_{2-x}\text{Sr}_x\text{CuO}_4$ ¹⁷ or by adding additional oxygen in $\text{YBa}_2\text{Cu}_3\text{O}_{6+x}$ ^{18,19}, the magnetic scattering moves out to incommensurate wavevectors, consistent with the stripe

ordering picture described above. This incommensurate magnetism can be either static or dynamic, as evidenced by either elastic or inelastic peaks in the neutron scattering respectively and now appears to be a common feature of the $\text{La}_{2-x}\text{Sr}_x\text{CuO}_4$ family of compounds. Specifically, for lightly doped $\text{La}_{2-x}\text{Sr}_x\text{CuO}_4$, elastic incommensurate magnetic Bragg features first appear split off from the $(0.5, 0.5)$ position in diagonal directions relative to a tetragonal unit cell^{20,21}. At higher doping in the underdoped superconducting regime, the peaks rotate by 45° to lie along directions parallel to the tetragonal axes or Cu-O-Cu bonds, such that elastic magnetic scattering appears at $(0.5 \pm \delta, 0.5, 0)$ and $(0.5, 0.5 \pm \delta, 0)$ ^{22,23}. For optimal and higher doping the static order disappears, but dynamic incommensurate correlations nevertheless persist^{23,24}.

Within the stripe picture, one expects charge ordering associated with the holes to occur at an incommensurate wavevector 2δ , twice that describing the spin order. Neutron scattering is not directly sensitive to charge ordering *per se*, but it is sensitive to atomic displacements, such as those associated with oxygen, which arise from charge ordering. An incommensurate nuclear scattering signature is therefore expected to appear at $(2 \pm 2\delta, 0, 0)$ or $(2, \pm 2\delta, 0)$ and related wavevectors. Despite extensive efforts, such incommensurate charge related scattering has not been observed in $\text{La}_{2-x}\text{Sr}_x\text{CuO}_4$ by either neutron or X-ray scattering techniques, although there is indirect evidence of charge stripe excitations from optical measurements²⁵. Such scattering *has* been observed in $\text{La}_{1.6-x}\text{Nd}_{0.4}\text{Sr}_x\text{CuO}_4$ ^{26,27}, as well as $\text{La}_{1.875}\text{Ba}_{0.125-x}\text{Sr}_x\text{CuO}_4$ ($x=0, 0.05, 0.06, 0.075, 0.085$)²⁸, motivating discussion as to whether such static charge stripes compete with, rather than underlie, high temper-

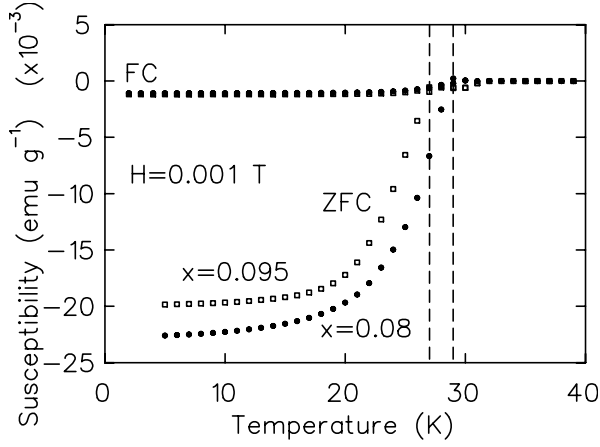


FIG. 1: Zero field cooled (ZFC) and field cooled (FC) susceptibilities of $\text{La}_{2-x}\text{Ba}_x\text{CuO}_4$ ($x=0.095$ and 0.08) single crystals measured at 0.001 T. Dashed lines indicate the onset of superconductivity at $T_C=27$ and 29 K for $x=0.095$ and $x=0.08$ samples respectively.

ature superconductivity. Surprisingly, $\text{La}_{2-x}\text{Ba}_x\text{CuO}_4$, the first high temperature superconductor (HTSC) to be discovered²⁹, has been much less extensively studied than either $\text{La}_{2-x}\text{Sr}_x\text{CuO}_4$ or $\text{YBa}_2\text{Cu}_3\text{O}_{6+x}$ due to the difficulty of growing single crystals, which has only been achieved³⁰ recently. In this paper, we report neutron scattering signatures of static incommensurate spin order in single crystal $\text{La}_{2-x}\text{Ba}_x\text{CuO}_4$ ($x=0.095, 0.08$), consistent with the stripe picture described above, but with interesting complexity not accounted for within present theoretical models. Our results clearly indicate that the spin ordering is insensitive to both the onset of superconductivity and surprisingly the application of a magnetic field. Tranquada *et al*³¹ and Fujita *et al*³² have reported neutron scattering measurements on an $x=0.125$ sample of $\text{La}_{2-x}\text{Ba}_x\text{CuO}_4$. In both $\text{La}_{2-x}\text{Ba}_x\text{CuO}_4$ and $\text{La}_{2-x}\text{Sr}_x\text{CuO}_4$ this concentration corresponds to a suppression of T_C as a function of doping, known as the “ $1/8$ ” anomaly. In $\text{La}_{2-x}\text{Ba}_x\text{CuO}_4$ the suppression is almost complete³³ and is associated with a structural phase transition at low temperature, from orthorhombic to tetragonal³⁷ which gives rise to a superlattice peak at $(0,1,0)$ and symmetry related reflections. Samples of $\text{La}_{2-x}\text{Ba}_x\text{CuO}_4$ near $x=0.125$ display a sequence of structures on lowering the temperature, going progressively from high temperature tetragonal (HTT, $I4/mmm$ symmetry) to orthorhombic (MTO, $bmab$ symmetry) to low temperature tetragonal (LTT, $P4_2/ncm$ symmetry)³⁷. The high temperature tetragonal to orthorhombic transition in particular, and to a lesser extent, the orthorhombic to low temperature tetragonal transition are sensitive indicators for the precise Ba doping level in the material.

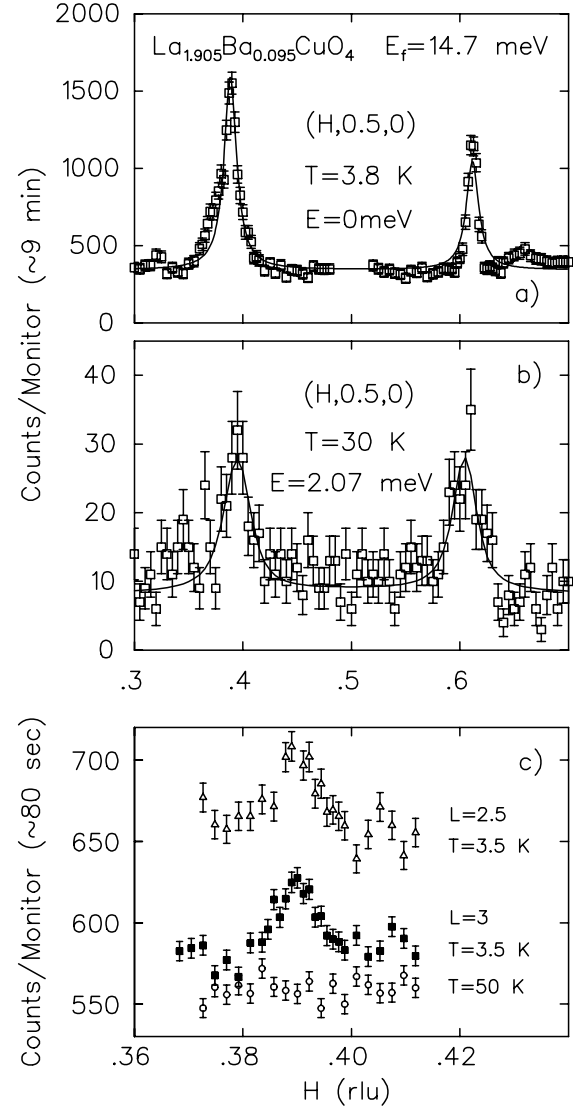


FIG. 2: a) Static incommensurate magnetic peaks with $\delta=0.112$ in $\text{La}_{1.905}\text{Ba}_{0.095}\text{CuO}_4$ at $T=3.8$ K, along $(H,0.5,0)$. b) Representative inelastic scans at $T=30$ K, also along $(H, 0.5, 0)$ and at $\hbar\omega= 2.07$ meV. Parameters characterizing this inelastic scattering are shown in Fig. 4, while the solid line is discussed in the text. c) Elastic scans of the form $(H, H/(1-2\delta), L)$, which demonstrate the rod-like, two dimensional nature of the elastic magnetic scattering, as described in the text. The scan at $L=2.5$ has been displaced by 50 counts upwards for clarity.

I. SINGLE CRYSTAL GROWTH, CHARACTERIZATION AND EXPERIMENTAL PROCEDURE

We have grown³⁴ high quality single crystals of $\text{La}_{2-x}\text{Ba}_x\text{CuO}_4$ with $x=0.095$ and $x=0.08$ using floating zone image furnace techniques with a four-mirror optical furnace. A small single crystal of La_2CuO_4 was employed as a seed for the growth, which was performed under enclosed pressures of 165 and 182 kPa of O_2 gas for

TABLE I: Summary of $\text{La}_{2-x}\text{Ba}_x\text{CuO}_4$ structural (T_{d1} , T_{d2}), superconducting (T_C) and magnetic (T_N) phase transition temperatures³⁴

x	T_{d1} (K)	T_{d2} (K)	T_C (K)	T_N (K)
0.125	232	60	$\sim 4^a$	50
0.095	272	45	27	39.5
0.08	305	35	29	39

^aFrom ³².

$x=0.095$ and $x=0.08$ samples respectively. The resulting ~ 6 gram single crystals of $\text{La}_{2-x}\text{Ba}_x\text{CuO}_4$ were cylindrical in shape and cut to dimensions 25 mm in length by 5 mm in diameter ($x=0.095$) and 38 mm in length by 5 mm diameter ($x=0.08$). We have determined the Ba concentration from the HTT to MTO transition temperature. The $\text{La}_{2-x}\text{Ba}_x\text{CuO}_4$ ($x=0.095$) and ($x=0.08$) single crystals displayed HTT to MTO structural phase transitions at $T_{d1} \sim 272$ K and $T_{d1} \sim 305$ K, respectively, and MTO to LTT transitions at $T_{d2} \sim 45$ K and $T_{d2} \sim 35$ K, respectively³⁴. The bulk superconducting transition temperatures $T_C = 27$ K ($x=0.095$) and $T_C = 29$ K ($x=0.08$) are identified using the onset of the zero field cooled diamagnetic response of the crystals, as measured using Superconducting Quantum Interference Device (SQUID) magnetometry and shown in Fig. 1. The various structural and superconducting phase transition temperatures are summarised in Table 1, along with the corresponding values for the $\text{La}_{2-x}\text{Ba}_x\text{CuO}_4$ ($x=0.125$) sample³².

Oxygen stoichiometry in $\text{La}_{2-x}\text{Ba}_x\text{CuO}_{4+y}$ is more difficult to quantify, especially at the low levels relevant here. Experience with $\text{La}_{2-x}\text{Sr}_x\text{CuO}_{4+y}$ suggests the oxygen stoichiometry, y , is negative in as-grown samples, giving rise to crystals which possess an effective doping level which is lower than that given by the Sr concentration alone; the effective doping level is $x + 2y$ ³⁵. Stoichiometric samples at optimal and underdoped Sr concentrations display a maximum superconducting T_C which cannot be increased by controlled annealing in O_2 gas. Excess oxygen can be incorporated into LaCuO_{4+y} crystals, but only through electrochemical doping methods, in which case y can be as high as 0.11 and the interstitial oxygen organizes itself into staged structures³⁶.

Neutron scattering experiments were undertaken on the C5 and N5 triple axis spectrometers at the Canadian Neutron Beam Centre, Chalk River. All experiments were performed with pyrolytic graphite (002) planes as monochromator and analyser, with constant $E_f = 14.7$ meV. A graphite filter was placed in the scattered beam to reduce contamination from higher order neutrons. The single crystals were oriented with (H,K,0) in the horizontal scattering plane. Crystallographic indices are denoted using tetragonal notation, where the basal plane lattice constant $a = 3.78$ Å at low temperatures.

II. ELASTIC NEUTRON SCATTERING IN $\text{La}_{2-x}\text{Ba}_x\text{CuO}_4$ ($x=0.095$)

A. Meissner State

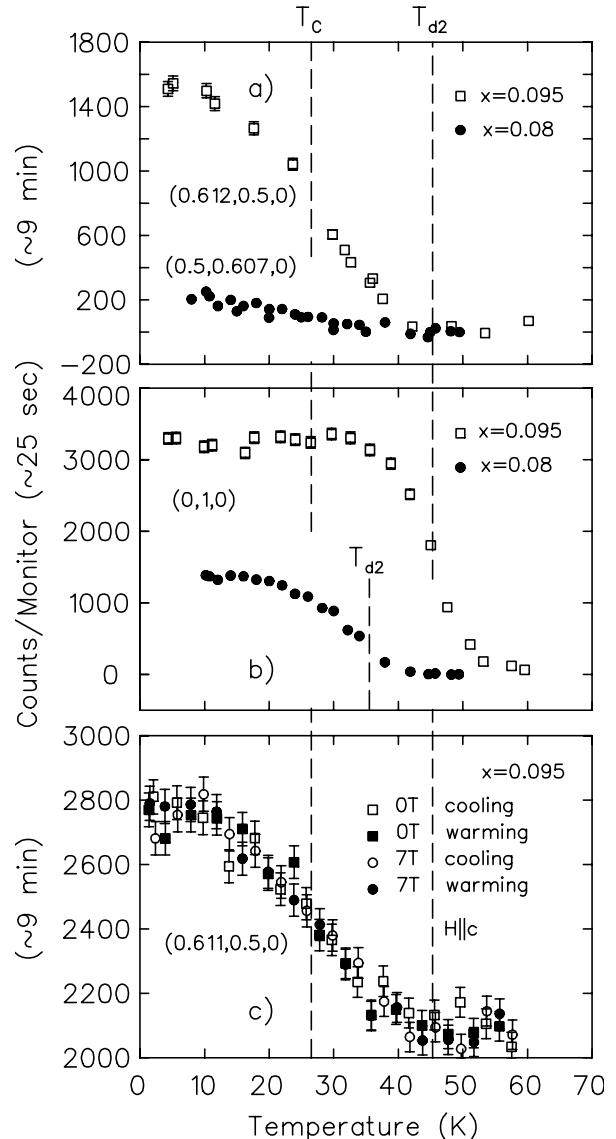


FIG. 3: a) The temperature dependence of the net elastic incommensurate magnetic scattering in $\text{La}_{2-x}\text{Ba}_x\text{CuO}_4$ ($x=0.095$) at $(0.612, 0.5, 0)$ and ($x=0.08$) at $(0.5, 0.607, 0)$, as well as that of b) the $(0, 1, 0)$ structural Bragg peak, which marks the orthorhombic to low temperature tetragonal structural phase transition. Note that a constant background has been subtracted in both cases. The superconducting and structural phase transition temperatures are indicated by dashed lines for both samples. All the data for $x=0.08$ have been scaled to the volume of the $x=0.095$ sample by phonon normalization. The counting times refer to the unscaled $x=0.095$ data. c) Temperature dependence of the elastic incommensurate magnetic scattering in $\text{La}_{2-x}\text{Ba}_x\text{CuO}_4$ ($x=0.095$) in 0 and $H=7$ T \parallel c.

We discuss the more extensive measurements on the $\text{La}_{2-x}\text{Ba}_x\text{CuO}_4$ sample with $x=0.095$ first. Elastic scattering scans at $T=3.8$ K are shown in Fig 2a), in which Bragg peaks occur at $(0.5\pm\delta, 0.5, 0)$ $\delta = 0.112(3)$, indicating static incommensurate spin order. Analogous magnetic Bragg peaks are observed at $(0.5, 0.5\pm 0.112, 0)$. All peak widths are resolution limited with full widths at half maximum, $\text{FWHM}=0.011 \text{ \AA}^{-1}$, indicating static spin correlations within the basal plane exceeding 180 \AA . By contrast, the spin correlations between planes are very short. To observe this, the crystal was reoriented in the (H, H, L) scattering plane and then tilted $\sim 7^\circ$ at constant L to intersect the incommensurate peak position for $H=0.39$. Measurements along H of the form $(H, H/(1-2\delta), L)$ at fixed L for $L=2.5$ and 3 are shown in Fig. 2c at $T=3.5$ K and at $L=3$ for $T=50$ K to extract a background. Since the peak intensity is independent of L , the scattering taking the form of an elastic rod along the L direction, the static spin order at low temperatures is two dimensional. Note that the intensity in Fig. 2a) is greater relative to that in Fig. 2c) for the sample oriented in the $(H, K, 0)$ plane. This arises because the neutron spectrometer has a broad vertical resolution which integrates the signal in the L direction, perpendicular to the scattering plane.

The temperature dependence of the incommensurate magnetic elastic scattering is illustrated in Fig. 3a. The intensity of the magnetic Bragg peak is proportional to the volume average of the square of the ordered staggered moment. The spin order at $(0.612, 0.5, 0)$ develops continuously with temperature below $T_N=39.5\pm 0.3$ K. The temperature dependence of the $(0, 1, 0)$ structural Bragg peak indicates the orthorhombic to low temperature tetragonal phase transition occurs at $T_{d2}\sim 45$ K, a transition which is discontinuous in nature³⁷. For reference, the superconducting transition at $T_C\sim 27$ K (see Fig. 1) is also indicated on this plot as a dashed line. The onset of spin ordering, T_N correlates most strongly with the completion of the transition to the low temperature tetragonal phase, and the incommensurate spin order coexists with the superconductivity below T_C . Associated incommensurate charge ordering has not been observed. The temperature dependence of the spin ordering is qualitatively similar to that observed in the $x=1/8$ compound³², where the superlattice peak intensity becomes non-zero below ~ 50 K. Similarly, no anomaly has been observed at T_C in $\text{YBCO}_{6.35}$ in the spin order, which has been attributed to robust spin correlations¹⁹.

B. Magnetic Field Dependence

The most surprising result of this study is that the incommensurate spin structure shows no magnetic field dependence up to 7 T, applied vertically along the c^* axis. Neither cooling nor warming the sample in a magnetic field has an effect on either the temperature dependence of the spin ordering, or the Bragg intensity in

$\text{La}_{2-x}\text{Ba}_x\text{CuO}_4$ ($x=0.095$), as shown in Fig. 3c. This result is in marked contrast with the behaviour of underdoped and optimally doped $\text{La}_{2-x}\text{Sr}_x\text{CuO}_4$ where pronounced field dependent effects are observed. For the optimally doped $\text{La}_{2-x}\text{Sr}_x\text{CuO}_4$ compound ($x=0.163$), the application of a magnetic field enhances the dynamical spin susceptibility but does not induce static order³⁸. Most dramatically, in a slightly underdoped sample ($x=0.144$), Khaykovich *et al*³⁹ report the development of a static incommensurate spin structure above a critical field of 2.7 T. The authors therefore argue that $\text{La}_{2-x}\text{Sr}_x\text{CuO}_4$ ($x=0.144$) may be tuned through a quantum critical point, at which there is a magnetic field induced transition between magnetically disordered and ordered phases. Their results are interpreted in terms of a Ginzburg-Landau model due to Demler *et al*⁴⁰, which assumes a microscopic competition between spin and superconducting order parameters. The predicted magnetic intensity increases as $\Delta I \sim H/H_{c2} \ln(H_{c2}/H)$ ⁴⁰, which is consistent with experiments on $\text{La}_{2-x}\text{Sr}_x\text{CuO}_4$. Note that the intensity changes most rapidly with magnetic field at low fields on a scale set by H_{c2} . In the $\text{La}_{2-x}\text{Ba}_x\text{CuO}_4$ family of compounds, the lower critical field is $H_{c1} \sim 0.04$ T, while the upper critical field H_{c2} is in excess of 40 T ⁴¹. The upper critical field is of the same order of magnitude in optimally doped $\text{La}_{2-x}\text{Sr}_x\text{CuO}_4$ ⁴². Thus an applied magnetic field of 7 T should be sufficiently large to see an effect in $\text{La}_{2-x}\text{Ba}_x\text{CuO}_4$.

For sufficiently underdoped $\text{La}_{2-x}\text{Sr}_x\text{CuO}_4$ ($x=0.12, 0.10$), the ordered magnetic moment associated with preexisting static spin order is enhanced on application of a magnetic field^{43,44,45}. The spin order within the vortex state of $\text{La}_{2-x}\text{Sr}_x\text{CuO}_4$ ($x=0.10$)⁴⁴ indicates long in-plane correlation lengths, greater than both the superconducting coherence length and the intervortex spacing at 14.5 T. As the coherence length is a measure of the size of the vortices, Lake *et al* argue the static magnetism must therefore reside beyond the extent of the vortices themselves⁴⁴. Whereas the $\text{La}_{2-x}\text{Ba}_x\text{CuO}_4$ ($x=0.095$) correlation length for static spin order is similarly long, the underlying physics is clearly different and the spins appear to order independent of vortex creation.

III. INELASTIC NEUTRON SCATTERING IN $\text{La}_{2-x}\text{Ba}_x\text{CuO}_4$ ($x=0.095$)

The magnetic excitations were studied in constant energy transfer scans performed through the incommensurate ordering wavevectors. Horizontal collimation sequences of $0.54^\circ\text{-}0.48^\circ\text{-S-}0.54^\circ\text{-}1.2^\circ$ and $0.54^\circ\text{-}0.79^\circ\text{-S-}0.85^\circ\text{-}2.4^\circ$ were used at energy transfers of 2.07 and 3.1 meV respectively, yielding corresponding energy resolutions of ~ 1 and ~ 1.5 meV FWHM. The representative scan along $(H, 0.5, 0)$ and $\hbar\omega=2.07$ meV at $T=30$ K in Fig. 2b, shows that the low energy dynamic spin response peaks up at the same wavevector, $(0.5\pm 0.112, 0.5, 0)$, as

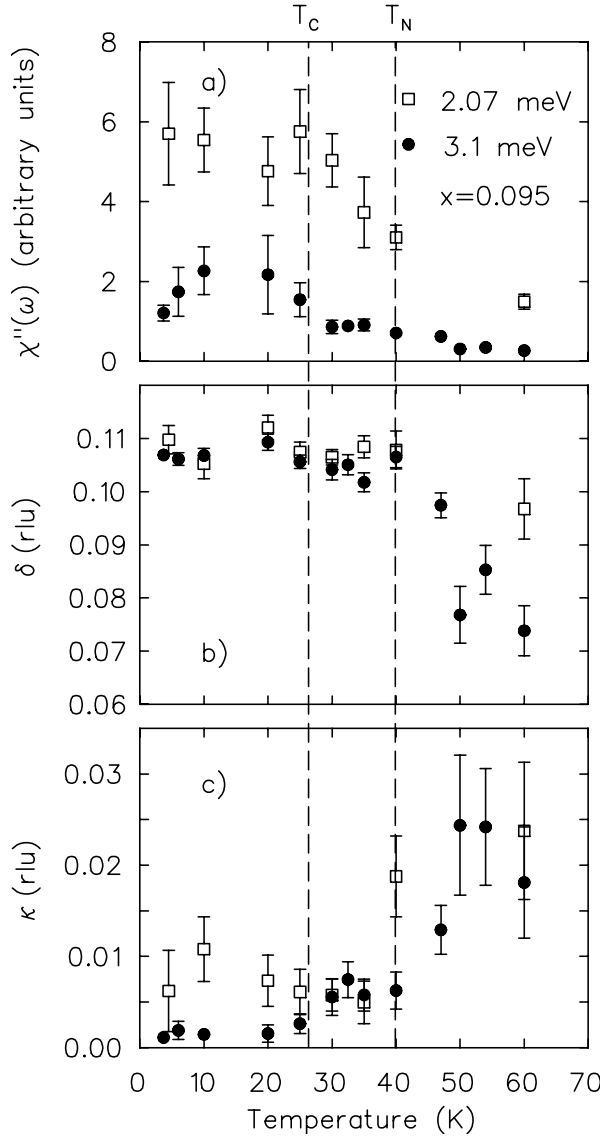


FIG. 4: The temperature dependence of the parameters extracted from fitting the low energy inelastic magnetic scattering shown in the middle panel of Fig. 2. This scattering was fit to Eq. 1, and we show (top panel) $\chi''(\mathbf{Q}, \hbar\omega=2.07$ and 3.1 meV); (middle panel) the incommensurability δ ; and (lower panel) the inverse correlation length κ . The dashed lines indicate the superconducting ($T_C \approx 27$ K) and magnetic ($T_N=39.5 \pm 0.3$ K) transition temperatures.

the static spin structure. At higher energy transfers the signal declines rapidly. The measured dynamic structure factor $S(\mathbf{Q}, \omega)$ is related to the imaginary part of the dynamical susceptibility $\chi''(\mathbf{Q}, \omega)$ through the fluctuation-dissipation theorem. For quantitative analysis, the data have been fit to the resolution convolution of $S(\mathbf{Q}, \omega) = \chi''(\mathbf{Q}, \omega)[1 - e^{-\hbar\omega/k_B T}]^{-1}$ where the susceptibility³² is:

$$\chi''(\mathbf{Q}, \hbar\omega) = \chi''(\hbar\omega) \sum_{n=1}^4 \frac{\kappa}{(\mathbf{Q} - \mathbf{Q}_{\delta,n})^2 + \kappa^2} \quad (1)$$

and $\mathbf{Q}_{\delta,n}$ represents the four incommensurate wave vectors $(\frac{1}{2} \pm \delta, \frac{1}{2}, 0)$ and $(\frac{1}{2}, \frac{1}{2} \pm \delta, 0)$. This assumes the magnetic excitations consist of four rods of scattering running along the c^* axis. The extracted temperature dependences of $\chi''(\hbar\omega)$, δ and κ are plotted in Figs. 4a, b and c respectively. $\chi''(\hbar\omega)$ is proportional to the integral of $\chi''(\mathbf{Q}, \omega)$ over \mathbf{Q} in the $(H, K, 0)$ scattering plane; δ is the incommensurability, while κ is the inverse of the static correlation length in the basal plane, defined as the peak half width at half maximum. For reference, both the spin ordering transition at $T_N \sim 39.5 \pm 0.3$ K, and the superconducting transition near $T_C \sim 27$ K are indicated on this plot. At both 2.07 meV and 3.1 meV, the dynamical susceptibility, $\chi''(\hbar\omega)$, increases continuously as the temperature is reduced below ~ 60 K, becoming roughly constant and non-zero below $T_C \sim 27$ K. This is similar to measurements in both overdoped $\text{La}_2\text{CuO}_{4+y}$, where a levelling off of the dynamic incommensurate spin response has been reported below $T_C \sim 42$ K⁴⁷ and also in $\text{La}_{2-x}\text{Ba}_x\text{CuO}_4$ ($x=0.125$) in the normal state³². In the latter compound, as a function of frequency there is relatively little change in $\chi''(\hbar\omega)$ at low temperature (8 K), whereas it drops rapidly in the present $x=0.095$ sample. As the temperature is raised, $\chi''(\hbar\omega)$ varies linearly with frequency at lower energy transfers below 10 meV in the $x=0.125$ sample for $T > 65$ K, whereas it declines with increasing ω in $x=0.095$ for all $T < 60$ K. Note that the signal intensity has been corrected for the monitor sensitivity to higher order incident neutrons, as described in Ref.¹⁸. These low energy excitations have some characteristics of the spin waves observed in the parent compound La_2CuO_4 ⁴⁸ as one warms through the Néel temperature, where instantaneous spin correlations with the character of the Néel state persist into the paramagnetic regime⁴⁹.

The form of $\chi''(\hbar\omega)$ varies dramatically as a function of doping in the related $\text{La}_{2-x}\text{Sr}_x\text{CuO}_4$ compounds. In optimally and slightly overdoped $\text{La}_{2-x}\text{Sr}_x\text{CuO}_4$ ($x=0.15, 0.18$)^{50,51} there is a characteristic energy of ~ 7 meV below which the dynamic susceptibility is dramatically reduced in the superconducting state - the opening up of a spin gap. However, on the underdoped side of the superconducting dome there is finite spectral weight in the spin response at all low energy transfers^{52,53}.

The bottom two panels of Fig 4 show that the incommensurability, δ and the inverse correlation length, κ , correlate most strongly with the disappearance of the static spin order near $T_N \sim 39$ K, which is not surprising. Above T_N the increase in κ may indicate that stripe correlations are weakened by thermal fluctuations that broaden the hole distribution about antiphase domain boundaries.

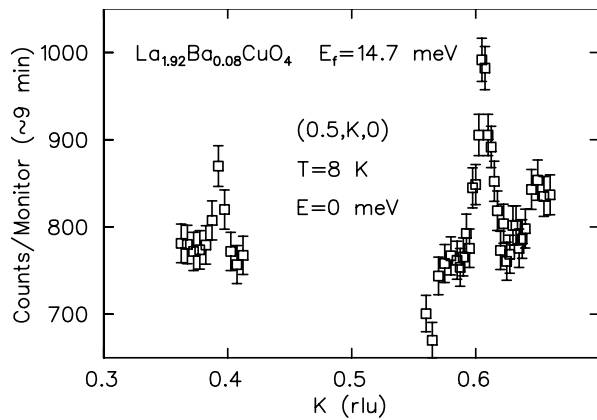


FIG. 5: Static incommensurate magnetic peaks with $\delta=0.107$ in $\text{La}_{1.92}\text{Ba}_{0.08}\text{CuO}_4$ at $T=8$ K, along $(0.5, K, 0)$.

IV. ELASTIC NEUTRON SCATTERING IN $\text{La}_{2-x}\text{Ba}_x\text{CuO}_4$ ($x=0.08$)

Qualitatively, the magnetic and superconducting properties of $\text{La}_{2-x}\text{Ba}_x\text{CuO}_4$ ($x=0.08$) ($T_C=29$ K) are very similar to those of the higher doped $x=0.095$ ($T_C=27$ K) sample. Elastic neutron scattering measurements were carried out under the same conditions as described earlier, with the single crystal oriented with (H, K, O) in the horizontal scattering plane. The elastic scattering scans at $T=8$ K (see Fig. 5) show that the incommensurate wave vector has decreased from $\delta = 0.112(3)$ in the $x=0.095$ sample to $0.107(3)$. Surprisingly, the magnetic scattering is roughly a factor of eight less intense (Fig. 3a). In Figs. 3a) and b) the intensities have been scaled to the sample volume using the integrated intensity of an acoustic phonon measured near a strong nuclear Bragg peak at $(2, 0.15, 0)$. We do not understand the reduced intensity for $x=0.08$, since extinction does not play a role.

The temperature dependence of the elastic magnetic signals at the incommensurate wavevectors $(0.5, 0.607, 0)$ for $\text{La}_{2-x}\text{Ba}_x\text{CuO}_4$ ($x=0.08$) and at $(0.612, 0.5, 0)$ for $\text{La}_{2-x}\text{Ba}_x\text{CuO}_4$ ($x=0.095$) are reproduced in Fig. 6, where the intensities have been scaled so that their functional form may be directly compared. As can be seen, both the temperature dependence of the order parameter and the phase transition temperatures are very similar despite the difference in the strength of the elastic magnetic Bragg scattering. We therefore conclude the two electronic energy scales for these crystals at $x=0.08$ and $x=0.095$, set by the superconducting T_C and T_N , are surprisingly similar. It is not clear why a 4% decrease in δ should produce an eight-fold decrease in the spin Bragg intensity. A search revealed no additional magnetic intensity in diagonal directions. As in $x=0.095$, no incommensurate peaks due to charge ordering were observed in the $x=0.08$ sample.

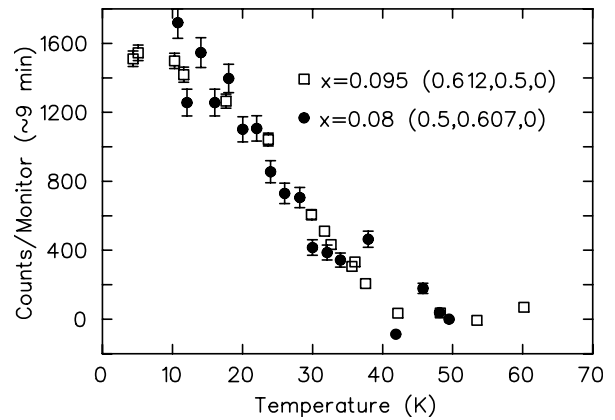


FIG. 6: The temperature dependence of the elastic incommensurate magnetic scattering in $\text{La}_{2-x}\text{Ba}_x\text{CuO}_4$ ($x=0.095$) at $(0.612, 0.5, 0)$ and ($x=0.08$) at $(0.5, 0.607, 0)$. The net intensity for $x=0.08$ has been multiplied by a factor of 7.7 to match that of $x=0.095$.

V. DISCUSSION

Whether magnetism and superconductivity coexist in the same microscopic regions of the CuO_2 planes or are phase separated is a topical subject of research. The issue of microscopic spatial segregation has been examined using a combination of neutron scattering⁴⁶ and μSR ⁵⁵ techniques in LaCuO_{4+y} . As a local probe μSR is sensitive to heterogeneous structures. The magnetic ordering in LaCuO_{4+y} ($y=0.11$) and $\text{La}_{2-x}\text{Sr}_x\text{CuO}_4$ ($x=0.12$) has been reported to occur in reduced magnetic volume fractions of 40 and 18% respectively⁵⁵. Khaykovich *et al* argue an applied magnetic field enhances spin ordering primarily in the nonmagnetic regions⁴⁶, consistent with the above observations. By contrast, the magnetic volume fraction in $\text{La}_{2-x}\text{Ba}_x\text{CuO}_4$ ($x=0.095$) is much larger, approaching 100%⁵⁶. We speculate that no magnetic field dependence has been observed in $\text{La}_{2-x}\text{Ba}_x\text{CuO}_4$ $x=0.095$ because the non-magnetic volume fraction is too low. A systematic study of the variation of the spin ordering with magnetic field is therefore of interest, with emphasis on the correlations between this effect and the magnetic volume fraction.

An interesting difference between the $x=0.08$ and the 0.095 $\text{La}_{2-x}\text{Ba}_x\text{CuO}_4$ samples is that the spin ordered state in the $x=0.095$ sample grows within a fully developed LTT structure, as $T_N \sim 39.5$ K and $T_{d2} \sim 45$ K. By contrast, in the $x=0.08$ $\text{La}_{2-x}\text{Ba}_x\text{CuO}_4$ sample, the MTO to LTT structural phase transition begins near T_N on decreasing temperature and is only completed at temperatures below ~ 20 K. The situation for $x=0.125$ $\text{La}_{2-x}\text{Ba}_x\text{CuO}_4$ is similar to the $x=0.095$ case, as $T_N \sim 50$ K, at which temperature the MTO-LTT transition for $x=0.125$ is largely complete. The first order nature of the MTO-LTT structural phase transition implies co-existing structures over the temperature regime at which the spin order forms for $x=0.08$ $\text{La}_{2-x}\text{Ba}_x\text{CuO}_4$. It is then possi-

ble that the resulting structural heterogeneity interferes with the full development of spin order, giving rise to a substantially reduced magnetic Bragg intensity as compared with the $x=0.095$ sample. However, we also note that variability⁴⁴ in the elastic magnetic Bragg intensity has been reported from $\text{La}_{2-x}\text{Sr}_x\text{CuO}_4$ sample to sample with similar nominal doping levels of $x \sim 0.1$ and the $\text{La}_{2-x}\text{Sr}_x\text{CuO}_4$ system does not display the LTT phase at low temperatures.

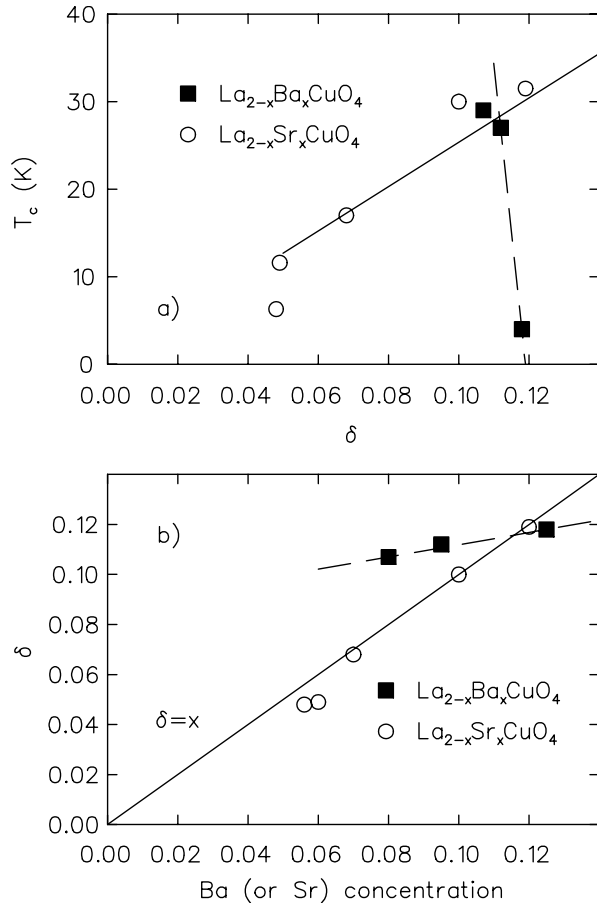


FIG. 7: a) Superconducting T_C is plotted vs elastic incommensuration, δ , for the $x=0.08$, 0.095 , and 0.125 $\text{La}_{2-x}\text{Ba}_x\text{CuO}_4$ samples, compared with those measured in related $\text{La}_{2-x}\text{Sr}_x\text{CuO}_4$ samples. b) Incommensurability δ is plotted vs Ba-content, x , for our $x=0.08$, $x=0.095$ $\text{La}_{2-x}\text{Ba}_x\text{CuO}_4$ samples, with previous $x=0.125$ $\text{La}_{2-x}\text{Ba}_x\text{CuO}_4$ results³² and those relevant to several underdoped $\text{La}_{2-x}\text{Sr}_x\text{CuO}_4$ samples^{23,54}. The dotted line is a guide to the eye.

It is also interesting to examine the correlation between Ba-content, x , incommensurability, δ , and superconducting T_C in $\text{La}_{2-x}\text{Ba}_x\text{CuO}_4$ and compare these relationships to those reported for $\text{La}_{2-x}\text{Sr}_x\text{CuO}_4$. The top panel of Fig. 7 shows T_C vs δ for the $x=0.08$, 0.095 , and 0.125 $\text{La}_{2-x}\text{Ba}_x\text{CuO}_4$ samples, compared with those measured in related $\text{La}_{2-x}\text{Sr}_x\text{CuO}_4$ samples. As can be seen, our results for the $x=0.08$ and $x=0.095$ samples give the same T_C as $\text{La}_{2-x}\text{Sr}_x\text{CuO}_4$ for the same incommensuration,

δ . Of course, $\text{La}_{2-x}\text{Ba}_x\text{CuO}_4$ displays the pronounced $x=1/8$ anomaly and consequently the $x=0.125$ point on this T_C vs δ plot lies far below the linear curve which is an excellent descriptor for the remainder of the underdoped $\text{La}_{2-x}\text{Ba}_x\text{CuO}_4$ and $\text{La}_{2-x}\text{Sr}_x\text{CuO}_4$ systems. The abrupt nature of the $x=1/8$ anomaly in the LBCO system is clear.

The bottom panel of Fig. 7 shows the incommensurability δ vs Ba-content, x and once again we compare our new results on $x=0.08$ and $x=0.095$ $\text{La}_{2-x}\text{Ba}_x\text{CuO}_4$ samples with the $x=0.125$ $\text{La}_{2-x}\text{Ba}_x\text{CuO}_4$ results and those of several underdoped $\text{La}_{2-x}\text{Sr}_x\text{CuO}_4$ samples at Sr concentrations above $x=0.05$, where the incommensurate spin ordering is consistent with a picture of parallel (as opposed to diagonal) stripe ordering. In this Sr-content regime, δ tracks x well, assuming stoichiometric oxygen content^{20,21,23,35}. One can see that the incommensuration in $x=0.08$ and $x=0.095$ $\text{La}_{2-x}\text{Ba}_x\text{CuO}_4$ shows relatively little x -dependence. Indeed, we observe δ values which are only $\sim 9\%$ less than that displayed by $x=0.125$ $\text{La}_{2-x}\text{Ba}_x\text{CuO}_4$, thereby departing significantly from the approximately linear δ vs x relation characterizing the underdoped $\text{La}_{2-x}\text{Sr}_x\text{CuO}_4$ studies.

It is possible that this difference between underdoped $\text{La}_{2-x}\text{Ba}_x\text{CuO}_4$ and $\text{La}_{2-x}\text{Sr}_x\text{CuO}_4$ also arises due to the MTO-LTT structural phase transition, occurring in $\text{La}_{2-x}\text{Ba}_x\text{CuO}_4$ but absent in $\text{La}_{2-x}\text{Sr}_x\text{CuO}_4$. It is also conceivable that it arises due to some small oxygen off-stoichiometry, such that our samples have the composition $\text{La}_{2-x}\text{Ba}_x\text{CuO}_{4+y}$, with oxygen stoichiometry greater than 4. Such excess oxygen would give rise to an effective hole doping given by $x_{eff} = x + 2y$. To bring the δ values for $x=0.08$ and 0.095 back onto the linear relationship between δ and x_{eff} seen in $\text{La}_{2-x}\text{Sr}_x\text{CuO}_4$, small, but positive values of y : 0.013 and 0.0075 for the $x=0.08$ and $x=0.095$ $\text{La}_{2-x}\text{Ba}_x\text{CuO}_{4+y}$ samples respectively would be required. This is too small to be detectable and runs counter to what is concluded in $\text{La}_{2-x}\text{Sr}_x\text{CuO}_{4+y}$. In underdoped $\text{La}_{2-x}\text{Sr}_x\text{CuO}_{4+y}$, the superconducting T_C is maximized by annealing in oxygen, at which point the measured δ vs Sr concentration, x , lie on the straight line³⁵. Consequently, as grown $\text{La}_{2-x}\text{Sr}_x\text{CuO}_{4+y}$ tends to be oxygen deficient ($y < 0$) and annealing in oxygen results in stoichiometric $\text{La}_{2-x}\text{Sr}_x\text{CuO}_4$. This is also expected to be true for underdoped $\text{La}_{2-x}\text{Ba}_x\text{CuO}_{4+y}$, which would imply that the deviation of δ vs x from a linear relationship is intrinsic to stoichiometric $\text{La}_{2-x}\text{Ba}_x\text{CuO}_4$, a surprising result.

VI. SUMMARY AND CONCLUSIONS

We have observed the coexistence of static, two dimensional incommensurate spin order and superconductivity in $\text{La}_{2-x}\text{Ba}_x\text{CuO}_4$ with $x=0.095$ and $x=0.08$. This result is in broad agreement with other well studied high temperature La-214 cuprate superconductors, such as $\text{La}_{2-x}\text{Sr}_x\text{CuO}_4$ or $\text{La}_2\text{CuO}_{4+y}$, which show signatures of

either incommensurate static spin ordering or dynamic spin correlations. One significant finding of this study is the field *independence* of the incommensurate magnetic order in the $x=0.095$ sample, in marked contrast with other superconducting La-214 cuprates. Studies of the spin ordering as a function of magnetic field in other superconducting systems with large magnetic volume fractions should prove illuminating. In addition, while the dependence of the superconducting T_C on the incommensuration of the magnetic structure, δ , in $\text{La}_{2-x}\text{Ba}_x\text{CuO}_4$ ($x=0.08, 0.095$) is the same as that observed in $\text{La}_{2-x}\text{Sr}_x\text{CuO}_4$, the x -dependence appears to be substantially weaker than that seen in $\text{La}_{2-x}\text{Sr}_x\text{CuO}_4$,

where a linear relationship is observed over this range of concentration. Now that crystal growth breakthroughs have resulted in the availability of large, high quality single crystals of $\text{La}_{2-x}\text{Ba}_x\text{CuO}_4$, fuller experimental characterization of the original family of high temperature superconductors is clearly warranted.

This work was supported by NSERC of Canada. It is a pleasure to acknowledge the contributions of A. Kallin, A. Dabkowski and E. Mazurek at McMaster, who were involved in the single crystal growth and characterization and the expert technical support of L. McEwan and R. Sammon at NRC, Chalk River.

-
- ¹ M. A. Kastner *et al*, Rev Mod Phys **70**, 897 (1998).
 - ² J. M. Tranquada, cond-mat/0512115 (2005).
 - ³ R.J. Birgeneau, C.Stock, J.M. Tranquada, K.Yamada, J Phys Soc Jpn (2006).
 - ⁴ A. H. Castro Neto and C. Morais Smith, in *Strong Interactions in Low Dimensions*, edited by D. Baeriswyl and L. Degiorgi (Kluwer Academic Publishing, 2004).
 - ⁵ S. Mori, C.H. Chen, S.W. Cheong, Nature **392**, 473 (1998); Phys. Rev. Lett. **81**, 3972 (1998);
 - ⁶ C. Renner *et al*, Nature **416**, 518 (2002).
 - ⁷ J. M. Tranquada, D.J. Buttrey, V. Sachan, and J.E. Lorenzo, Phys. Rev. Lett. **73**, 1003 (1994); S-H. Lee and S-W. Cheong, Phys. Rev. Lett. **79**, 2514 (1997); H. Yoshizawa *et al*, Phys. Rev. B **61**, R854 (2000).
 - ⁸ C-H. Du *et al*, Phys. Rev. Lett. **84**, 3911 (2000).
 - ⁹ Y. Yoshinari, P.C. Hammel, and S.W. Cheong, Phys. Rev. Lett. **82**, 3536 (1999).
 - ¹⁰ T. Katsufuji, T. Tanabe, T. Ishikawa, Y. Fukuda, T. Arima, and Y. Tokura, Phys. Rev. B **54**, R14230 (1996); G. Blumberg, M.V. Klein, and S.W. Cheong, Phys. Rev. Lett. **80**, 564 (1998); K. Yamamoto, T. Katsufuji, T. Tanabe, and Y. Tokura, Phys. Rev. Lett. **80**, 1493 (1998).
 - ¹¹ N. Bulut, D. Hone, D. J. Scalapino, N. E. Bickers, Phys Rev Lett **64**, 2723 (1990).
 - ¹² N. Bulut, D. J. Scalapino, Phys Rev B **53**, 5149 (1996).
 - ¹³ M. R. Norman, Phys Rev B **61**, 14751 (2000).
 - ¹⁴ S. A. Kivelson *et al*, Rev Mod Phys **75**, 1201 (2003).
 - ¹⁵ D. Vaknin *et al*, Phys Rev Lett **58**, 2802 (1987).
 - ¹⁶ J.M. Tranquada *et al*, Phys Rev Lett **60**, 156 (1988)
 - ¹⁷ K. Yamada *et al*, Phys. Rev. B **57**, 6165 (1998); H. Kimura *et al*, Phys. Rev. B **59**, 6517 (1999).
 - ¹⁸ C. Stock, W.J.L. Buyers, R.Liang, D. Peets, Z. Tun, D. Bonn, W.N. Hardy, and R.J. Birgeneau, Phys. Rev. B, **69**, 014502 (2004).
 - ¹⁹ C. Stock, W. J. L. Buyers, Z. Yamani, C. L. Broholm, J. -H. Chung, Z. Tun, R. Liang, D. Bonn, W. N. Hardy, R. J. Birgeneau, Phys. Rev. B **73**, 100504(R) (2006).
 - ²⁰ M. Matsuda *et al*, Phys. Rev. B **62**, 9148 (2000);
 - ²¹ S. Wakimoto *et al*, Phys. Rev. B **61**, 3699 (2000).
 - ²² T. Suzuki, T. Goto, K. Chiba, T. Shinoda, T. Fukase, H. Kimura, K. Yamada, M. Ohashi, Y. Yamaguchi, Phys Rev B **57**, R3229 (1998).
 - ²³ H. Kimura, K. Hirota, H. Matsushita, K. Yamada, Y. Endoh, S-H Lee, C. F. Majkrzak, R. Erwin, G. Shirane, M. Greven, Y. S. Lee, M. A. Kastner and R. J. Birgeneau, Phys Rev B **59**, 6517 (1999).
 - ²⁴ S. Wakimoto *et al*, Phys Rev Lett, **92** 217004 (2004).
 - ²⁵ A. Lucarelli *et al*, Phys. Rev. Lett. **90**, 037002 (2003).
 - ²⁶ J. M. Tranquada, B. J. Sternlieb, J. D. Axe, Y. Nakamura, S. Uchida, Nature **375**, 561 (1995).
 - ²⁷ J. M. Tranquada, J. D. Axe, N. Ichikawa, A. R. Moodenbaugh, Y. Nakamura, S. Uchida, Phys Rev Lett **78**, 338 (1997).
 - ²⁸ M. Fujita, H. Goka, K. Yamada, M. Matsuda, Phys Rev B, **66** 184503 (2002).
 - ²⁹ J.G. Bednorz and K.A. Muller, Z. Phys B **64**, 189 (1986).
 - ³⁰ T. Adachi, T. Noji, and Y. Koike, Phys Rev B **64**, 144524 (2001).
 - ³¹ J.M Tranquada, H. Woo, T.G. Perring, H. Goka, G.D. Gu, G. Xu, M. Fujita, and K. Yamada, Nature, **429**, 534 (2004).
 - ³² M. Fujita, H. Goka, K. Yamada, J. M. Tranquada, L. P. Regnault, Phys Rev B **70**, 104517 (2004).
 - ³³ A. R. Moodenbaugh, Y. Xu, M. Suenaga, T. Folkerts, and R. Shelton, Phys Rev B **38**, 4596 (1988).
 - ³⁴ Y. Zhao *et al*, arXiv:0707.2799 (2007).
 - ³⁵ K. Yamada, C. H. Lee, K. Kurahashi, J. Wada, S. Wakimoto, S. Ueki, H. Kimura, Y. Endoh, S. Hosoya, G. Shirane, R. J. Birgeneau, M. Greven, M. A. Kastner, and Y. J. Kim, Phys Rev B **57**, 6165 (1998).
 - ³⁶ Y. S. Lee, F. C. Chou, A. Tewary, M. A. Kastner, S. H. Lee and R. J. Birgeneau, Phys. Rev. B **69**, 020502(R) (2004)
 - ³⁷ J. D. Axe *et al*, Phys Rev Lett **62**, 2751 (1989).
 - ³⁸ B. Lake *et al*, Science **291**, 1759 (2001).
 - ³⁹ B. Khaykovich, S. Wakimoto, R. J. Birgeneau, M. A. Kastner, Y. S. Lee, P. Smeibidl, P. Vorderwisch, K. Yamada, Phys Rev B **71**, 220508 (2005).
 - ⁴⁰ E. Demler, S. Sachdev, Y. Zhang, Phys Rev Lett **87**, 067202 (2001).
 - ⁴¹ H. Takagi *et al*, J. J. Applied Phys. **26**, L434 (1987).
 - ⁴² G. S. Boebinger, Y. Ando, A. Passner, T. Kimura, M. Okuya, J. Shimoyama, K. Kishio, K. Tamasaku, N. Ichikawa and S. Uchida, Phys. Rev. Lett. **77**, 5417 (1996).
 - ⁴³ S. Katano, M. Sato, K. Yamada, T. Suzuki, T. Fukase, Phys Rev B **62**, R14677 (2000).
 - ⁴⁴ B. Lake *et al*, Nature **415**, 299 (2002).
 - ⁴⁵ B. Lake, K. Lefmann, N. B. Christensen, G. Aeppli, D. F. McMorrow, H. M. Ronnow, P. Vorderwisch, P. Smeibidl, N. Mangkorntong, T. Sasagawa, M. Nohara, H. Takagi, Nature Materials **4**, 658 (2005).

- ⁴⁶ B. Khaykovich, Y. S. Lee, R. W. Erwin, S.-H. Lee, S. Wakimoto, K. J. Thomas, M. A. Kastner and R. J. Birgeneau, *Phys Rev B* **66**, 014528 (2002).
- ⁴⁷ Y. S. Lee, R. J. Birgeneau, M. A. Kastner, Y. Endoh, S. Wakimoto, K. Yamada, R. W. Erwin, S.-H. Lee, G. Shirane, *Phys. Rev. B* **60**, 3643 (1999).
- ⁴⁸ K. Yamada, K. Kakurai, Y. Endoh, T. R. Thurston, M. A. Kastner, R. J. Birgeneau, G. Shirane, Y. Hidaka, T. Murakami, *Phys Rev B* **40**, 4557 (1989).
- ⁴⁹ G. Shirane, Y. Endoh, R. J. Birgeneau, M. A. Kastner, Y. Hidaka, M. Oda, M. Suzuki, and T. Murakami, *Phys. Rev. Lett.* **59**, 1613 (1987).
- ⁵⁰ K. Yamada, S. Wakimoto, G. Shirane, C. H. Lee, M. A. Kastner, S. Hosoya, M. Greven, Y. Endoh, R. J. Birgeneau, *Phys Rev Lett* **75**, 1626 (1995).
- ⁵¹ K. Yamada, C. H. Lee, Y. endoh, G. Shirane, R. J. Birgeneau, M. A. Kastner, *Physica C* **282-287**, 85 (1997)
- ⁵² Chul-Ho Lee, Kazuyoshi Yamada, Yasuo Endoh, Gen Shirane, R. J. Birgeneau, M. A. Kastner, M. Greven, Y-J. Kim, *J. Phys. Soc Jpn* **69**, 1170 (2000).
- ⁵³ Haruhiro Hiraka, Yasuo Endoh, Masaki Fujita, Young S. Lee, Jiri Kulda, Alexandre Ivanov, Robert J. Birgeneau, *J. Phys Soc Jpn* **70**, 853 (2001).
- ⁵⁴ M. Fujita, K. Yamada, H. Hiraka, P. M. Gehring, S. H. Lee, S. Wakimoto and G. Shirane, *Phys Rev B* **65**, 064505 (2002).
- ⁵⁵ A. T. Savici, Y. Fudamoto, I. M. Gat, T. Ito, M. I. Larkin, Y. J. Uemura, G. M. Luke, K. M. Kojima, Y. S. Lee, M. A. Kastner, R. J. Birgeneau, K. Yamada, *phys Rev B* **66**, 014524 (2002).
- ⁵⁶ S. R. Dunsiger *et al*, (unpublished).